

# Atomic spirograph : Quantum state measurement using coherent transients

Antoine Monmayrant, Béatrice Chatel, and Bertrand Girard  
*Laboratoire Collisions, Agrégats, Réactivité (UMR 5589 CNRS-UPS), IRSAMC,  
Université Paul Sabatier Toulouse 3, 31062 Toulouse cedex 9, France*

(Dated: February 9, 2020)

We present the principle and experimental demonstration of Time Resolved Quantum State Holography. The quantum state of an excited state interacting with an ultrashort chirped laser pulse is measured during this interaction. This has been obtained by manipulating coherent transients created by the interaction of femtosecond shaped pulses and rubidium atoms.

PACS numbers: 32.80.Qk, 42.50Md, 82.53.Kp

Quantum state measurement is a central issue of fundamental importance to quantum mechanics [1, 2]. Since only probabilities can be predicted by quantum mechanics, the phases of the wave function seem at first sight meaningless. However, relative phases between quantum states are crucial in many circumstances such as prediction of the free or driven evolution of the system, or the measurements of quantities (observables) related to the superposition of quantum states with different energies.

Several examples of quantum phase measurements of states created by ultrashort pulses are based on interferences between an unknown wave function and a "reference" wave function. These wave functions are created by a sequence of two ultrashort pulses (an unknown pulse and a reference pulse). In quantum state holography, the quantum state created by the unknown pulse is deduced either by time- and frequency- integrated fluorescence measured as a function of the delay [3, 4], or by measuring the population of each eigenstate for different values of the relative phases [5], or the amplitude of fluctuations when the delay is randomly fluctuating [6, 7]. In fluorescence tomography, position probability distributions are measured as a function of time [8, 9]. For instance, the dispersed fluorescence emitted by an oscillating nuclear wave packet in a diatomic molecule provides the position distribution through the Franck-Condon principle [8]. Alternatively the induced dipole can be obtained from heterodyne measurement [10]. More recently the internuclear quantum state of dissociating molecules have been elegantly measured by tomography using velocity map imaging [11].

In all these examples, the quantum state is first prepared and then measured in a second step. In the work reported here, the quantum state is measured *during* the interaction with the unknown laser pulse. Its evolution is thus recorded in real time.

When the matter - light interaction is in the linear regime, the final state populations can be entirely deduced from the power spectrum. This is for instance the case for a one-photon transition in the weak field regime. However, the phase of the wave function is sensitive to the various phases of the electric field. This can have important consequences for applications where a subsequent excitation is performed, in particular when coherent superpositions are involved.

The transient evolution of excited state population is also strongly dependent on the detailed laser shape. In particular, non-resonant contributions are as important as resonant ones. As an intuitive illustration of this statement, the transient response to a non-resonant excitation follows the electric field temporal envelope, independently of its spectrum. For instance, simply changing the pulse duration changes this transient response.

A resonant interaction leads to radically different behaviors. Fourier Transform (FT) limited pulses produce a step-wise excitation in the weak-field regime, and Rabi oscillations in the intermediate and strong field regime. Chirped pulses produce a total population inversion in the strong field with a final state robust with respect to small variations of laser parameters [12]. Chirped pulses in the weak field regime lead to Coherent Transients (CTs) [13, 14], a less intuitive behavior which illustrates the relative importance of the various stages of the interaction. The laser frequency sweeps linearly with time and crosses the resonance. Most of the population transfer occurs at resonance. The small fraction of excited state amplitude transferred after resonance leads to strong oscillations due to interferences between the oscillating atomic dipole and the exciting field (see Fig. 1, dotted line). Otherwise, interaction before resonance results in negligible effects. Similarly, in propagation experiments, interferences between the field radiated by the atom and the incoming field leads to interferences which can be used as a partial analysis of the field such as chirp [15] or dispersion [16] measurements.

The shape of these CTs can be radically changed by using a pulse shaper [17, 18]. This high sensitivity of Coherent Transients to slight modifications of the laser pulse provides possibilities to use CT measurements as a characterization of the laser pulse itself [19] or of the quantum state which is generated. In a simple approach, if the general shape of the laser pulse is known and only few parameters need to be determined, one can use a simple adjustment of these parameters to fit the experimental CTs with the predicted ones [18]. However, one would like to establish a general method providing a direct inversion from the data to the quantum state. One limitation of CTs is that only the part of the pulse after resonance leads to oscillations which can be used to determine the shape. Another difficulty is that the mea-

sured quantity is related to the excited state probability whereas one aims to measure probability amplitudes. In this contribution we show how it is possible to overcome these difficulties. Several CT measurements are combined, each with a sequence of two pulses. This sequence consists of a reference pulse which creates an initial population in the excited state, and an "unknown" pulse whose effect on the quantum state is to be measured in real time. The first pulse creates an initial population in the excited state so that the corresponding dipole beats with the whole of the second (unknown) pulse. A second measurement is performed after adding a  $\pi/2$  phase shift to the second pulse. This provides in-phase and in-quadrature measurements from which the real-time evolution (*during the laser interaction*) of the quantum state can be deduced. In common with quantum state holography [3], the quantum state created by the unknown pulse is determined by direct interferometric comparison with a reference quantum state. However, in our method, the unknown quantum state is measured at any time during and after its creation. Moreover, the properties of the first pulse need not be fully characterized in our method.

Consider the resonant interaction between an atomic system and a sequence of two weak nonoverlapping femtosecond laser pulses  $\mathcal{E}_1(t)$  and  $\mathcal{E}_2(t)$ . First order time dependent perturbation theory predicts the probability of finding the atom in the excited state at any time  $\tau$  after the interaction with the first pulse to be

$$\begin{aligned} S^\theta(\tau) &= |a_{e1}(\infty) + e^{i\theta}a_{e2}(\tau)|^2 \\ &= |a_{e1}(\infty)|^2 + |a_{e2}(\tau)|^2 + 2 \operatorname{Re} [e^{i\theta}a_{e1}^*(\infty)a_{e2}(\tau)] \end{aligned} \quad (1)$$

Here  $\theta$  is an arbitrary phase which can be added to the second pulse with respect to the first one. The probability amplitude produced by the pulse  $\mathcal{E}_k(t)$  is

$$a_{ek}(t) = -\frac{\mu_{eg}}{2i\hbar} \int_{-\infty}^t \mathcal{E}_k(t') e^{i\omega_{eg}t'} dt' \quad (2)$$

where  $\omega_{eg}$  is the transition frequency and  $\mu_{eg}$  the dipole moment matrix element. The excited state probability  $S^\theta(\tau)$  can be measured in a pump-probe scheme with an ultrashort probe pulse tuned on a transition towards another excited state  $|f\rangle$  [14]. The probability amplitude produced by the second pulse  $a_{e2}(t)$  can be obtained by resolving the nonlinear equation array resulting from a set of two experiments performed with different values of  $\theta$ . For instance,  $\theta_0$  and  $\theta_0 + \pi/2$  can be chosen. If the second pulse is much weaker than the first one, the quadratic term in  $a_{e2}(\tau)$  can be neglected to obtain a simple linear equation array. Alternatively, a third measurement can be performed with only the second pulse in order to measure  $|a_{e2}(\tau)|^2$  directly.

The two pulse sequence with a well defined phase relationship can be generated at once by a pulse shaper [20]. For this purpose, the complex spectral mask

$$H_\theta(\omega) = \{1 + \exp[i(\theta + \phi'\Delta\omega + \phi''(\Delta\omega)^2/2)]\}/2 \quad (3)$$

is applied to modify the electric field. Here  $\Delta\omega = \omega - \omega_L$ , where  $\omega_L$  is the laser carrier frequency. The first pulse is short (FT limited) and the second one is delayed and strongly chirped in order to produce the CTs. The first pulse creates the required initial excited population to produce oscillations during the whole second pulse as shown on Fig. 1.

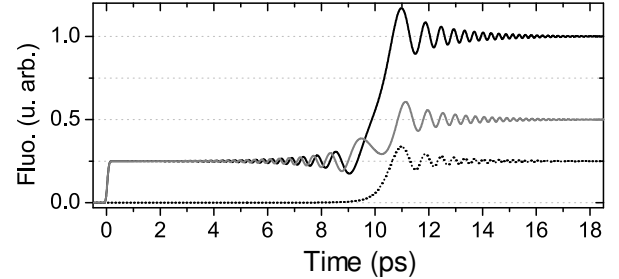


FIG. 1: Simulation of Coherent Transients resulting from the excitation of the atom by a FT limited pulse (at time  $t=0$ ) followed by a chirped pulse (centered at  $t=10$ ps). For  $\theta = 0$  (black) and  $\theta = \pi/2$  (gray). Dotted line: "Simple" CTs obtained for a single pulse at  $t=10$ ps.

To illustrate this scheme, an experiment has been performed in atomic rubidium. The experimental set-up is displayed in Fig. 2. The  $5s-5p(P_{1/2})$  transition (at

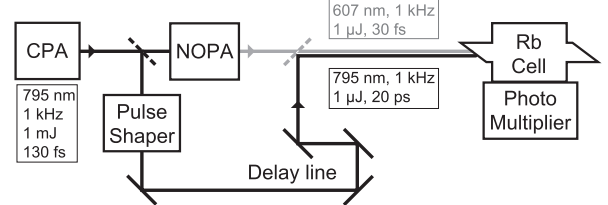


FIG. 2: Experimental set-up. NOPA : non collinear optical parametric amplifier; CPA: Chirped Pulse Amplifier

795 nm) is resonantly excited with a pulse sequence. The transient excited state population is probed "in real time" on the  $5p-(8s, 6d)$  transitions with an ultrashort pulse (at 607 nm). The laser system is based on a conventional Ti:Sapphire laser with chirped pulse amplification (Spitfire, Spectra Physics) which supplies 1 mJ -130 fs -795 nm pulses. Half of the beam is used for the pump pulse. The remaining half seeds a home made Non-collinear Optical Parametric Amplifier (NOPA) compressed using double pass silica prisms, which delivers pulses of a few microJoule, 30 fs -FWHM pulse intensity, centered around 607 nm. The pump pulse is shaped with a programmable pulse-shaping device[20], recombined with the probe pulse and sent into a sealed rubidium cell. The pump-probe signal is detected by monitoring the fluorescence at 420 nm due to the radiative cascade (8s, 6d) - 6p - 5s collected by a photomultiplier tube as a function of the pump-probe delay. The pulse

shaping device is a 4f set-up composed of one pair each of reflective gratings and cylindrical mirrors. Its active elements -two 640 pixels liquid crystal masks- are installed in the common focal plane of both mirrors. This provides high resolution pulse shaping in both phase and amplitude [20]. This is used to generate the shaped pump pulse by applying the function  $H_\theta$  defined above. The laser is centered at resonance ( $\omega_L = \omega_{eg}$ ). The delay between the two pulses is equal to  $\phi' = 6$  ps. The second pulse is strongly chirped ( $\phi'' = -2.10^5$  fs<sup>2</sup>) to around 10 ps duration.

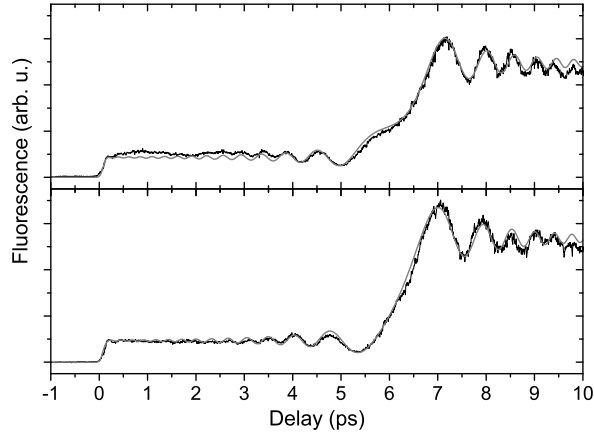


FIG. 3: Coherent Transients resulting from the excitation of the atom by a FT limited pulse (at time  $t=0$ ) followed by a chirped pulse (centered at  $t=6$  ps). Lower panel: relative phase between pulses  $\theta = \theta_0 \simeq -0.7$  rad and upper panel :  $\theta = \theta_0 + \pi/2$ . Solid line : theory; squares : experiment.

Figure 3 displays the Coherent Transients obtained with the two experiments performed with  $\theta = \theta_0 \simeq -0.7$  rad and  $\theta = \theta_0 + \pi/2$ . The squares represent the experimental results which fit perfectly with the resolution of the Schrödinger equation (solid line). The first plateau (for positive times) is due to the population induced by the first FT limited pulse. It allows  $|a_{e1}(\infty)|^2$  to be determined.

The effects of the second pulse can be divided into three parts. The strong increase taking place at resonance (around  $t = 6$  ps) is preceded and followed by oscillations resulting from interferences of off-resonance contributions with the resonant population. The height of the asymptotic value depends strongly on the relative phase  $\theta$ .

The excited state probability amplitude produced by the second pulse is extracted from the two measurements displayed in Fig. 3. The good stability of the laser allows the raw data to be used without any renormalization between the two pairs of measurements. The reconstructed probability amplitude is displayed on Fig. 4 in a 3D plot (complex plane as a function of time). The projections on

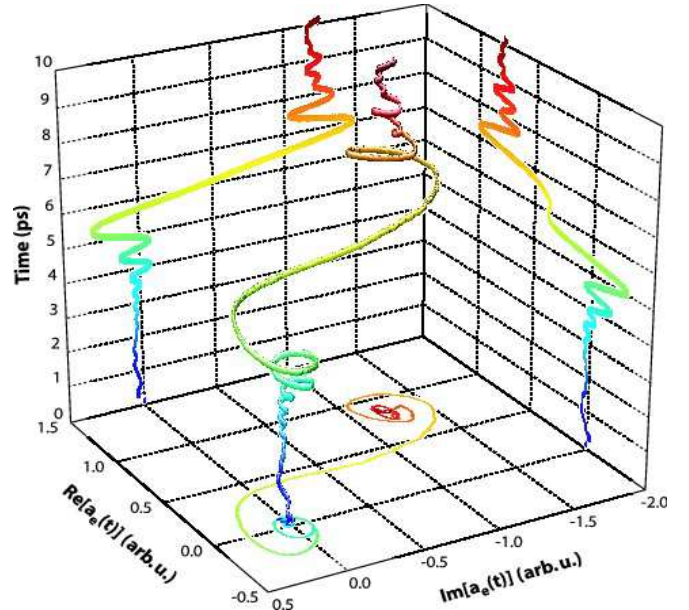


FIG. 4: Experimental probability amplitude reconstructed from the CTs of Fig. 3. Real part and Imaginary parts are shown as a function of time.

the various 2D planes are also displayed. The expected Cornu spiral is clearly seen in the complex plane.

The first part of the spiral winds around the population induced by the first pulse (which has been subtracted on the graph). After passage through resonance corresponding to an almost "straight" direction as expected (stationary phase in Eq. 2), the second part of the spiral winds around the asymptotic value resulting from the combined effects of both pulses. The reconstruction procedure requires resolving a set of nonlinear equations. Two solutions are in general mathematically obtained, but only one is physically acceptable. It is obtained by continuity from the solution corresponding to the beginning of the second pulse for which  $a_{e2}(-\infty) = 0$ . This procedure works efficiently as long as these two solutions are not degenerated. This may occur for particular values of  $\theta$  if the second pulse is larger than the first one. This situation should therefore be avoided. However, a scheme with three measurements as depicted above (see Fig. 1) could instead be used in this situation. Figure 5 gives examples of Cornu spirals reconstructed for  $\theta$  values of  $\theta_0 = 3.3$  rad and  $\theta_0 + 2\pi/3$ . for similar pulse amplitudes. The quality of the reconstruction is excellent in the two cases.

The present experiment benefits from the wide capability of our high resolution pulse shaper [20]. In particular it delivers a sequence of two shaped pulses with excellent (interferometric) stability. The lack of stability was a serious limitation (partly bypassed by measuring the noise induced by delay fluctuations [6, 21]) in previous experiments [22]. This was overcome only recently in Michelson type experiments [23, 24].

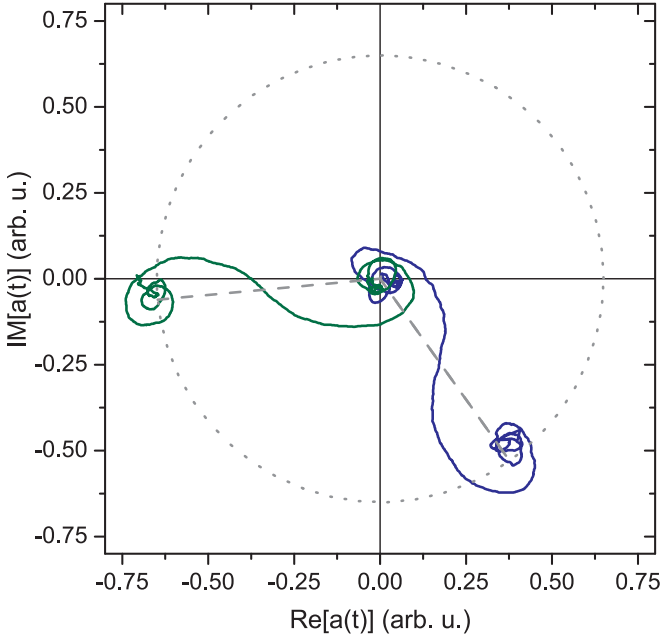


FIG. 5: Reconstructed experimental probability amplitude obtained for different values of the relative phase :  $\theta_0 = 3.3$  rad and  $\theta_0 + 2\pi/3$ .

The present scheme achieves time resolved measurement of a single quantum state. Extension to a superposition of quantum states is rather straightforward. The

phase and amplitude pulse shaper allows specific phases to be applied to the second pulse at the transition frequencies associated with each independent excited state. A simple scheme with  $(2p + 1)$  measurements for  $p$  excited states can be derived. This provides with a system of  $2p$  linear equations with  $2p$  unknowns (real and imaginary part of each probability amplitude). The set of specific phases can be easily chosen to ensure that the corresponding system can be inverted. Such a scheme would present an extension of quantum state holography [3, 4] to the time evolution holography of a complex quantum wave packet.

Weak-field interaction is not an intrinsic limitation of this technique which can be extended to wave packets created in the strong field. In this regime, iterative algorithms have been proposed to reconstruct the quantum state in wave packet interferences [25] and could be implemented in our scheme.

We have demonstrated how the instantaneous excited state can be reconstructed during its interaction with a laser pulse. This scheme is very general and can be used even without chirping the pulse. It can have wide applications in situations where careful control of the wave function during ultrashort pulses interaction is searched. This is in particular the case of quantum information applications. It can of course be also used to characterize complex pulse shapes [19].

We sincerely acknowledge Julien Courteaud for his help during a part of the experiment and Chris Meier for fruitful discussions.

---

[1] M. G. Raymer, *Contemp. Phys.* **38**, 343 (1997).  
[2] W. P. Schleich, *Quantum Optics in Phase Space* (Wiley-VCH, Berlin, 2001).  
[3] C. Leichtle, W. P. Schleich, I. S. Averbukh, and M. Shapiro, *Phys. Rev. Lett.* **80**, 1418 (1998).  
[4] I. S. Averbukh, M. Shapiro, C. Leichtle, and W. P. Schleich, *Phys. Rev. A* **59**, 2163 (1999).  
[5] X. Chen and J. A. Yeazell, *Phys. Rev. A* **56**, 2316 (1997).  
[6] T. C. Weinacht, J. Ahn, and P. H. Bucksbaum, *Phys. Rev. Lett.* **80**, 5508 (1998).  
[7] T. C. Weinacht, J. Ahn, and P. H. Bucksbaum, *Nature* **397**, 233 (1999).  
[8] T. J. Dunn, I. A. Walmsley, and S. Mukamel, *Phys. Rev. Lett.* **74**, 884 (1995).  
[9] U. Leonhardt and M. G. Raymer, *Phys. Rev. Lett.* **76**, 1985 (1996).  
[10] A. Zucchetti, W. Vogel, D. G. Welsch, and I. A. Walmsley, *Phys. Rev. A* **60**, 2716 (1999), article.  
[11] E. Skovsen, H. Stapelfeldt, S. Juhl, and K. Molmer, *Phys. Rev. Lett.* **91** (2003), article 090406.  
[12] B. Broers, H. B. van Linden van den Heuvell, and L. D. Noordam, *Phys. Rev. Lett.* **69**, 2062 (1992).  
[13] N. V. Vitanov, *Phys. Rev. A* **59**, 988 (1999).  
[14] S. Zamith, J. Degert, S. Stock, B. de Beauvoir, V. Blanchet, M. A. Bouchene, and B. Girard, *Phys. Rev. Lett.* **87**, 033001 (2001).  
[15] J. E. Rothenberg, *IEEE J. Quant. Electronics* **QE-22**, 174 (1986).  
[16] J. Delagnes, A. Monmayrant, P. Zahariev, B. Chatel, B. Girard, and M. A. Bouchene, *Appl. Phys. B* **submitted** (2005).  
[17] J. Degert, W. Wohlleben, B. Chatel, M. Motzkus, and B. Girard, *Phys. Rev. Lett.* **89**, 203003 (2002).  
[18] W. Wohlleben, J. Degert, A. Monmayrant, B. Chatel, M. Motzkus, and B. Girard, *App. Phys. B* **79**, 435 (2004).  
[19] A. Monmayrant, B. Chatel, and B. Girard, *Opt. Lett.* **accepted** (2005).  
[20] A. Monmayrant and B. Chatel, *Rev. Sci. Inst.* **75**, 2668 (2004).  
[21] O. Kinrot, I. Averbukh, and Y. Prior, *Phys. Rev. Lett.* **75**, 3822 (1995).  
[22] V. Blanchet, C. Nicole, M. A. Bouchene, and B. Girard, *Phys. Rev. Lett.* **78**, 2716 (1997).  
[23] K. Ohmori, Y. Sato, E. E. Nikitin, and S. A. Rice, *Phys. Rev. Lett.* **91**, 243003 (2003).  
[24] H. Katsuki, H. Chiba, B. Girard, C. Meier, and K. Ohmori, *Phys. Rev. Lett.* **submitted** (2005).  
[25] X. Chen and J. A. Yeazell, *Phys. Rev. A* **60**, 4253 (1999), article.